Chemical Geology 642 (2023) 121801

Contents lists available at ScienceDirect

Chemical Geology

journal homepage: www.elsevier.com/locate/chemgeo

Assessing hydrological controls on the lithium isotope weathering tracer

Philip A.E. Pogge von Strandmann [a,b,*], Lara R. Cosford [b], Chun-Yao Liu [b], Xianyi Liu [b], Alexander J. Krause [b], David J. Wilson [b], Xiaoqing He [a], Alex J. McCoy-West [c], Sigurður R. Gislason [d], Kevin W. Burton [e]

[a] MIGHTY, Institute of Geosciences, Johannes Gutenberg University, Mainz, Germany
[b] LOGIC, Department of Earth Sciences, University College London, London, UK
[c] IsoTropics Laboratory, Earth and Environmental Sciences, James Cook University, Townsville, QLD 4811, Australia
[d] Institute of Earth Sciences, University of Iceland, Reykjavik, Iceland
[e] Department of Earth Sciences, Durham University, Durham, UK

ARTICLE INFO

Editor: Christian France-Lanord

Keywords:
Silicate weathering
Basalt weathering
Secondary mineral formation
Clay formation
Weathering intensity

ABSTRACT

To investigate the impact of riverine discharge and weathering intensity on lithium isotopes (δ^7Li) in a mono-lithological terrain, this study examines the dissolved load and leached suspended load (exchangeable, oxide, and clay fractions) from Icelandic rivers spanning a wide range of discharge, weathering rates, and weathering intensity. The $\delta^7Li_{dissolved}$ co-varies inversely with the discharge, confirming that water-rock interaction time is a primary control on the secondary mineral formation that fractionates Li isotopes. The "boomerang" shape observed in global rivers between the weathering intensity (i.e. W/D = weathering rate/denudation rate) and $\delta^7Li_{dissolved}$ also exists for these basaltic rivers at low to medium W/D. However, these rivers do not extend to such low $\delta^7Li_{dissolved}$ values as seen in the global compilation at low W/D, indicating that there is a lithological control on this relationship arising from the type of the lithology-specific secondary minerals forming and their precipitation rates. In addition, the $\Delta^7Li_{x\text{-}dissolved}$ between each leached solid phase and the dissolved load also co-varies with discharge. At low discharge (long water-rock interaction times), $\Delta^7Li_{x\text{-}dissolved}$ values agree with experimentally-determined equilibrium values, whereas less fractionated values are observed at higher discharge (shorter water-rock interaction times). As a result, there is a different relationship between W/D and $\Delta^7Li_{clay\text{-}source}$ in this basaltic terrain than previously reported from global multi-lithological river sediment samples, with clay leachates from Iceland more closely mimicking the boomerang shape of the dissolved load. However, the relationship between δ^7Li and weathering processes is complicated because the fractionation between the clay fraction and the dissolved load is not constant but varies with both W/D and discharge. Overall, this study confirms the utility of Li isotopes as a tracer of modern and palaeo-weathering processes, and also has important implications for the specific interpretations of detrital δ^7Li values, which may be more sensitive to weathering parameters than previously thought.

1. Introduction

Chemical weathering of silicate rocks is considered to be a fundamental control on atmospheric CO_2 and long-term climate (Walker et al., 1981). During weathering, carbon from the atmosphere is dissolved and, together with cations such as Ca and Mg from silicate rock dissolution, is transported to the oceans, where it is ultimately sequestered as carbonate (Berner, 2003; Berner et al., 1983). In addition, chemical weathering provides significant nutrients to the oceans (e.g. Si, Fe, P), stimulating primary productivity, which takes up atmospheric carbon via photosynthesis. In general, almost all organic carbon produced in surface waters escapes burial and is re-oxidised, ultimately returning to the atmosphere (e.g. Hedges and Keil, 1995). However, weathering provides two additional pathways that increase organic carbon burial: 1) the formation of clay particles, on which algae grow as they leach nutrients, with the clay helping to bury the subsequent organic carbon (Grimm et al., 2019; Kennedy and Wagner, 2011); and 2) via the "rusty carbon sink", where Fe oxyhydroxides shield organic carbon from reoxidation (Lalonde et al., 2012). In summary, chemical weathering draws down atmospheric CO_2 via multiple inorganic and organic

* Corresponding author at: MIGHTY, Institute of Geosciences, Johannes Gutenberg University, Mainz, Germany.
E-mail address: ppoggevo@uni-mainz.de (P.A.E. Pogge von Strandmann).

https://doi.org/10.1016/j.chemgeo.2023.121801
Received 8 August 2023; Received in revised form 18 October 2023; Accepted 26 October 2023
Available online 29 October 2023

pathways, and on multiple timescales from tens of kyr (carbonate burial) to seasonal cycles (organic carbon fertilisation).

Hence, there is considerable interest in understanding weathering, both in the present day and in the geological record. Lithium isotope ratios (reported as δ^7Li values) are apparently insensitive to issues that affect many other potential weathering tracers. Specifically, Li isotopes are demonstrably not fractionated by primary productivity (Pogge von Strandmann et al., 2016), and although some recent studies have reported Li isotope fractionation in plants (Li et al., 2020), others dispute this finding (Clergue et al., 2015; Lemarchand et al., 2010; Steinhoefel et al., 2021). Regardless, the amount of Li taken up by plants is always very low, and has been shown to have a negligible effect on the Li isotope composition of surface waters (Pogge von Strandmann et al., 2021c). Furthermore, Li is present in silicates at several orders of magnitude higher concentrations than in carbonates, so Li isotopes trace silicate weathering, even in carbonate-dominated catchments (Kisakürek et al., 2005).

During natural weathering, primary silicate minerals dissolve without significant Li isotope fractionation (Pistiner and Henderson, 2003; Wimpenny et al., 2010). However, both the adsorption by and structural incorporation into secondary minerals (clays, oxyhydroxides) favour the lighter isotope ^{6}Li, leaving residual waters isotopically heavy (e.g. Huh et al., 2001; Pogge von Strandmann et al., 2021a). This has been demonstrated in both clay formation experiments (Hindshaw et al., 2019; Vigier et al., 2008), and weathering experiments. The latter reacted Icelandic basalt with water under different conditions, and observed decreases in [Li] and increases in δ^7Li_{diss}, due to very rapid (within a few hours) secondary mineral formation (Pogge von Strandmann et al., 2019b; Pogge von Strandmann et al., 2022). Steady-state fractionation values are reached within a few months. Sequential leaching of the reacted basalt showed that ~75% of Li was removed into clays, while the rest was taken up by oxides and the exchangeable fraction. Each of these phases had its own isotopic fractionation factor, but different clay types had identical fractionation factors (Pogge von Strandmann et al., 2022).

Recently, Zhang et al. (2022) produced a global compilation of seasonally-averaged river runoff (or discharge) and dissolved δ^7Li values (based on available time-series data), which showed a negative co-variation between the two parameters. They hypothesised that this relationship reflects greater water-rock interaction time (residence time) under lower runoff conditions, which allows for greater secondary mineral formation, more δ^7Li fractionation and consequently higher dissolved δ^7Li values. Similarly, other studies have reported a similar effect in a time-series of cave drip-waters (Wilson et al., 2021), and during a single storm event in California (Golla et al., 2022).

The degree of Li isotope enrichment in waters has been used as a tracer of the weathering intensity (that is, the ratio of the weathering rate to the denudation rate, W/D), with a relationship that is referred to as the "boomerang" curve (Bouchez et al., 2013; Dellinger et al., 2015). At low weathering intensity (highly erosive, kinetically-limited environments), the dissolution of primary minerals dominates, leading to limited fractionation of δ^7Li_{diss} from δ^7Li_{rock} values. At medium weathering intensity (floodplain environments), significant clay formation causes high δ^7Li_{diss} values, due to extensive isotopic fractionation. At high weathering intensity (supply-limited regimes), preformed secondary minerals (clays, but also potentially oxides) start to dissolve, releasing isotopically light Li so δ^7Li_{diss} values are low again but with a significantly lower Li yield and flux than evidenced at low W/D regimes (Dellinger et al., 2015; Pogge von Strandmann et al., 2021a). Reactive-transport models have been used to suggest that the low δ^7Li and high [Li] typically found at low W/D may be due to dissolution of a Li-rich mineral phase that is exposed by the high erosion rates (Winnick et al., 2022). However, those models were based on granitic weathering, where such phases (e.g. chlorite) are readily available. In basaltic weathering, as in this study, a single easy to dissolve, Li-rich mineral, is not present, and the initial phases to dissolve (i.e. glass, olivine and pyroxene) have similar [Li] and δ^7Li values (Brant et al., 2012; Wimpenny et al., 2010). The "boomerang" relationship between δ^7Li and W/D has also been used to calculate silicate weathering fluxes and/or rates through past climate events (e.g. Caves Rugenstein et al., 2019; Krause et al., 2023; Pogge von Strandmann et al., 2013; Pogge von Strandmann et al., 2021d; Sproson et al., 2022).

Dellinger et al. (2017) also produced a similar compilation of the Li isotope fractionation in the solid phases, between <0.6 μm (clay-sized) material in suspended river sediments and their source lithologies. In their compilation, the $\Delta^7Li_{clay\text{-}source}$ value was close to zero at low W/D values (the material largely being unaltered rock), whereas the fine-grained fraction was almost 10‰ lower than the source at very high W/D values (clay-rich rock). It should be noted that Dellinger et al. (2017) pointed out that their measured fine-grained fraction contained "non-negligible" amounts of unweathered primary material, which could have partly influenced their data, in particular for samples at low and medium W/D values. This may mean that part of the observed trend is due to mixing, with increasing amounts of isotopically light clays in each isotopically lighter sample, although this probably would not explain the δ^7Li variability observed in the fully weathered Amazon samples of Dellinger et al. (2017).

This study therefore has several motivations. First, both dissolved and clay Li isotope ratios have been proposed as different tracers of weathering intensity, based on compilations of global rivers (Dellinger et al., 2017; Dellinger et al., 2015). It remains unknown whether the type of rock undergoing weathering could affect the relationship between Li isotopes and weathering intensity, for example via changes to dissolution and clay formation rates.

Second, weathering studies of Iceland (Vigier et al., 2009) and Canada (Millot et al., 2010) have shown co-variations between dissolved Li isotope ratios and silicate weathering rates, which has also led to interpretations of the palaeo-record using these relationships (Dosseto et al., 2015). Although more recent studies have shown that such correlations might be special cases (Pogge von Strandmann et al., 2017a), these initial relationships are intriguing and are yet to be fully explained.

Finally, it has recently been suggested that the δ^7Li values in some large rivers (and also during a storm event) show a direct correlation with river discharge, which has been attributed to variations in water-rock interaction time (i.e. a long interaction time will enable more formation of secondary minerals, which fractionate Li isotopes) (Golla et al., 2022; Zhang et al., 2022). However, this hypothesis of a hydrological control on Li isotopes requires testing in mono-lithological catchments within the same climate zone, where other variables are more closely controlled.

In this study, we explore the above relationships by examining samples from a series of rivers in Iceland. Given that Iceland has a relatively simple basaltic weathering regime, and that many of its rivers are gauged and continuously monitored, it is well suited for delving into this behaviour. In addition, since Li isotopes in detrital silicate archives are increasingly being used as local palaeo-weathering records (Li et al., 2016; Pogge von Strandmann et al., 2017b; Pogge von Strandmann et al., 2021d; Wei et al., 2020), we also assess the fractionation between river water and secondary minerals (exchangeable, oxide, and clay fractions), and their relationship to discharge and weathering rates. In particular, the analyses of different phases of the suspended load, and their relationship to hydrological factors, has not been attempted before.

2. Field area and samples

The lithology of Iceland is dominated by basalt (~85%), with the oldest exposed rocks no older than ~14 Ma (Thordarson and Hoskuldsson, 2002). The overall geology is controlled by the volcanic zones that follow the SW-NE trend of the mid-Atlantic ridge, such that the basalts in the centre of the island are the youngest, and those in the NW and E are the oldest. Iceland has a cool temperate maritime climate, with a mean annual temperature of 4 °C in Reykjavik, and mean annual

precipitation of ~3000 mm on the south coast, ~1000 mm on the west coast, and < 400 mm in the central highlands. Around 11% of the island's area of 103,000 km^2 is glaciated, dominantly by four major icecaps, which reached their pre-industrial size approximately 8000 yr ago (Norddahl and Petursson, 2005).

Here we sampled a series of both direct-runoff and glacier-fed rivers from across Iceland (Fig. 1). The goal was to sample similar rivers to the study of Vigier et al. (2009), as well as those of another Icelandic weathering study (Louvat et al., 2008), and indeed a number of them are the same rivers as in those studies. We also focused on the Hvitá catchment in the west of Iceland, which runs into the Borgarfjörður fjord, because this system has been extensively studied for both Li and other isotope systems (Hindshaw et al., 2013; Jones et al., 2014; Pearce et al., 2010; Pogge von Strandmann et al., 2008; Pogge von Strandmann et al., 2006; Pogge von Strandmann et al., 2011a). Overall, the studied rivers sample virtually the entire range of dominantly basaltic surface bedrock in Iceland, with variations seen, for example, in the volcanic glass content (prevalent in younger rocks, and in subglacially-erupted rocks). However, as Li is a moderately incompatible element in magmatic processes, the variation of bedrock δ^7Li values across Iceland is very small (see Results).

3. Methods

3.1. Field methods

The river water samples were collected in July 2017. In the field, samples were generally collected from the centre of the river flow, mainly from bridges, in pre-cleaned containers. All rivers (except one sample, 07) were sampled at gauging sites of the Icelandic Meteorological Office, which provides continuously monitored discharge data. At each site the pH, temperature, and conductivity were measured. Alkalinity was immediately determined in the field by titration. To measure total suspended solids (TSS), a known quantity of water (50–250 ml, depending on the visible TSS amount) was filtered through a pre-weighed 0.2 μm filter, which was subsequently dried and re-weighed. Within 8 h, the remaining water was also filtered through 0.2 μm cellulose-acetate filters using a pressurised Teflon unit. The filters were stored and used to recover suspended material.

3.2. Leaching methods

In order to determine the composition of different phases within the suspended load (exchangeable, oxide, and clay), we employed a sequential extraction method that has previously been used and refined for Li isotopes, as detailed exhaustively elsewhere (Liu et al., 2022; Pogge von Strandmann et al., 2022). Briefly, the material was washed off the filters with Milli-Q water, and the exchangeable phase was extracted using 1 M Na acetate. The oxide phase was then leached using 0.04 M hydroxylamine hydrochloride (HH) in 25% *v*/v acetic acid. A clay leach was also applied, using 0.6 M HCl. This approach requires samples to have a surface passivation effect, whereby the secondary silicates are coating the original primary silicates, such as in river particles. Confidence in these leaching methods comes from basalt weathering experiments, which are able to close the Li mass balance when combining all leached phases (Liu et al., 2022; Pogge von Strandmann et al., 2019b; Pogge von Strandmann et al., 2014; Pogge von Strandmann et al., 2022). This clay leach is aimed at determining the Li isotope composition of the silicate secondary mineral (clay) fraction, but will likely not totally dissolve this fraction (Pogge von Strandmann et al.,

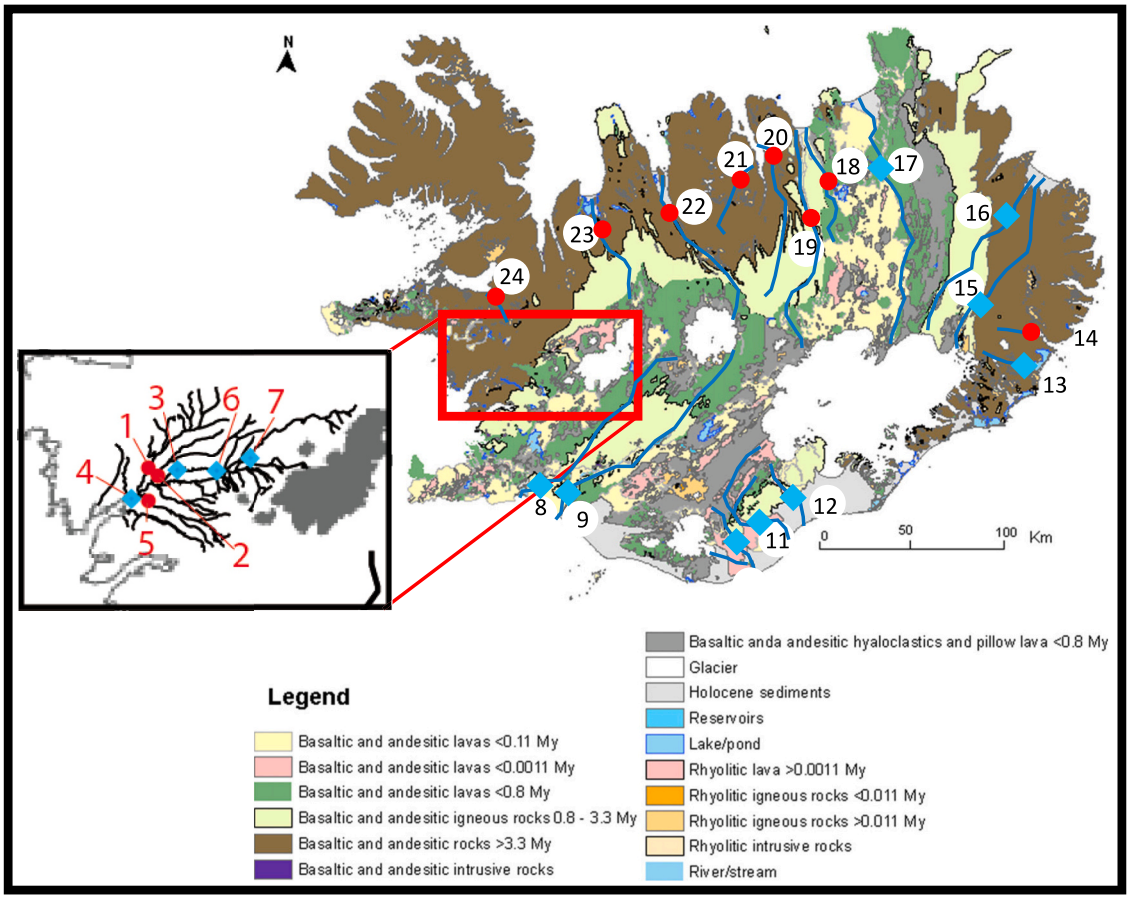

Fig. 1. Sample location map, with the geological map of Iceland modified from Oskarsdottir et al. (2011). The insert map from Borgarfjörður is modified from Pogge von Strandmann et al. (2006). Location symbols match those of Figs. 3, 5, 7, and 9: circles represent direct-runoff rivers, and diamonds represent glacier-fed rivers.

2019b). As such, while the δ^7Li values and elemental ratios of this leach have been shown to dominantly reflect secondary silicates, the absolute elemental amounts extracted only represent a minimum estimate. The bulk rock (i.e. suspended load sample that was not leached) was dissolved in stages of HF-HNO_3-$HClO_4$, followed by HNO_3, and HCl.

3.3. Concentrations

Anion concentrations were measured by ion chromatography, using a Thermo Scientific Dionex ICS 6000 at Durham University. For the waters, both major and trace elements were measured using a Varian 820-MS ICP-MS in the LOGIC laboratories at University College London. The analyses were calibrated using multi-element solutions mixed from single-element standards, and accuracy was assessed by analysing the international reference standard SLRS-5. The analytical reproducibility was better than ±6% (RSD) for all reported elements, and the measured values for SLRS-5 were within the uncertainty of the calibrated values, where available.

The cation concentrations of the sediment digestions and leaches were analysed using an Agilent 8900 triple-quad ICP-MS in the MIGHTY laboratories in Mainz. Calibration lines were constructed using combinations of single-element standards. For the bulk sediment digestions, the secondary standards used were the USGS basalt standards BCR-2 and BIR-1. For the leaches, the calibration solutions were matrix-matched to the leach (e.g. for the analyses of the exchangeable fraction, the calibration standards had a comparable high Na matrix). Reference standards do not exist for leachates, but leaches of the USGS standards BCR-2 and SGR-1b by these methods are reported in Liu et al. (2022).

3.4. Lithium isotope analyses

The methods for Li isotope purification and analyses are well established and documented at the LOGIC laboratories (e.g. Pogge von Strandmann et al., 2019b). Briefly samples were purified using a 2-stage cation exchange column method, using 0.2 M HCl as an eluant. Analyses were performed on a Nu Plasma 3, normalising to the IRMM-016 standard, which is isotopically indistinguishable from the LSVEC standard (Pogge von Strandmann et al., 2019b). Multiple water and rock standards have been analysed by these methods (Pogge von Strandmann et al., 2011b; Pogge von Strandmann et al., 2019b). Of relevance here are the analyses of USGS basalt standard BCR-2, with δ^7Li = 2.58 ± 0.32‰ (2sd; n = 11; dissolutions = 11), and of seawater, with δ^7Li = 31.18 ± 0.38 (2sd; n = 52). These values agree well with other publications (e.g. Jeffcoate et al., 2004), and show that the long-term external error (over >5 years) is ±0.4‰ (2sd).

4. Results

4.1. Physical measurements

The pH of Icelandic river waters tends to be controlled by 1) silicate weathering of Ca—Mg silicates, which consumes protons and drives pH higher; 2) the decay of organic matter, which drives pH lower; and 3) the precipitation of (non-oxide) secondary minerals, which also drives pH lower (Pogge von Strandmann et al., 2010). Glacial rivers and groundwaters tend to have high pH, due to their initial isolation from atmospheric CO_2 (Gislason and Eugster, 1987; Gíslason et al., 1996). In this study, the rivers exhibit a pH range of 6.4 to 9.6.

Total dissolved solids (TDS, determined via conductivity) range from 8.6 to 503 μg/ml, and total suspended solids (TSS) range from 0.1 to 44 mg/l, with higher TSS values found in glacier-fed waters, due to glaciers' high erosion capability. Alkalinity ranges from 0.14 to 1.25 meq/l. Discharge is also highly variable (2.9 to 503 m^3/s), and is highest in glacial rivers, and lowest in rivers that exhibit soil storage (see Section 5.3). Combining discharge with the catchment areas (Table S1) and the precipitation-corrected base cations + Si concentrations yields the chemical weathering rates, which range from 2.1 to 383 t/km^2/yr. Substituting the TSS values yields the physical erosion rates, which range from 77 to 964,000 t/km^2/yr. The very high erosion rates are found in glacier-fed rivers (which tend to have high discharge and high TSS) that were sampled close to the glacial snouts. Overall, this wide range in weathering and erosion rates leads to a wide range in weathering intensity (W/D = W/(W + E), where W is weathering rate, D is denudation rate, and E is erosion rate) from 0.0004 to 0.22. These values span a large part of the currently available global range in W/D studied for Li isotopes (0.003–0.7; Dellinger et al., 2015), and indeed considerably extend the range of W/D for rivers with Li isotope measurements to lower values, albeit they do not extend to the very high weathering intensity values observed in the Amazon Shield.

4.2. Dissolved load chemistry and Li isotopes

The major and trace element concentrations of the dissolved load are given in Table S2. In Iceland, both rainwater and surface ice melt have been shown to have seawater-like elemental ratios and δ^7Li values (plus other isotope ratios like Mg and Sr) (Hindshaw et al., 2013; Pogge von Strandmann et al., 2008; Pogge von Strandmann et al., 2006). We therefore conduct a precipitation correction, by assuming that all chloride (Cl^-) in the water samples stems from precipitation, and that the precipitation has elemental ratios and isotope compositions matching seawater. The corrected concentrations and isotope ratios are denoted by *. On average, 3% of dissolved Li for glacier-fed rivers and 9% of dissolved Li for direct-runoff rivers is derived from precipitation. This input leads to an average change in δ^7Li values of +0.4‰ (range from −0.18 to +2.5‰), which is small compared to the total riverine range of 10.9 to 36.6‰ for δ^7Li*.

Hydrothermal waters (i.e. hot groundwaters) can provide chemical inputs to streams close to the ridge axis in Iceland. They tend to have relatively high TDS and high [Li], and low δ^7Li values (Pogge von Strandmann et al., 2006; Pogge von Strandmann et al., 2016), and as such would have the tendency to apparently move rivers towards the low W/D endmember. Rivers with a known significant hydrothermal input in this sample set are the Skaftá (sample 11–2017-RW) and the Laxá (18–2017-RW, which drains the hydrothermally-sourced Lake Myvatn), and they also have slightly elevated SO_4^{2-} concentrations (Table S2; Pogge von Strandmann et al., 2006; Pogge von Strandmann et al., 2016). However, their δ^7Li values (21.5 and 20.1‰, respectively) are not noticeably different from nearby rivers with no known hydrothermal input. Therefore, we consider that hydrothermal inputs do not exert a major control on the dissolved Li isotope values in our dataset.

Considering the temperature range of these water samples (4.8–17.5 °C) (Table S1), a temperature-dependent control on the Li isotope fractionation factor between fluid and solid should theoretically cause up to ~2‰ variability in δ^7Li_{diss} values between samples (Li and West, 2014), which is small compared to the total 25.7‰ variation observed, and there is no overall co-variation between temperature and δ^7Li_{diss} values. Even individual river types show no co-variation: for example, the glacial rivers (4.8–11.7 °C) exhibit generally higher δ^7Li values at higher temperatures. This should be the other way round if temperature were a controlling factor.

Mineral saturation was calculated using the PHREEQC programme (Parkhurst and Appelo, 1999). Primary basaltic minerals, such as forsterite, plagioclase, and pyroxene are uniformly undersaturated in all water samples. Typical secondary silicates that form in Iceland, such as smectite and allophane, are mostly supersaturated, except in the samples at the lowest pH (6.4) and highest pH (9.6). Iron oxides, such as hematite, ferrihydrite and goethite, are always supersaturated. This behaviour is typical of Icelandic rivers (Eiriksdottir et al., 2013; Gíslason et al., 1996; Stefansson and Gislason, 2001).

4.3. Leachate chemistry and Li isotopes

To an extent, sequential leaches also leach phases other than those intended, at each step. We examine the possibility this occurred using elemental ratios (Table S3), as detailed extensively in Pogge von Strandmann et al. (2019a, 2019b, 2022) and Liu et al. (2022). For example, Si, as a neutral species, should not be significantly associated with the exchangeable fraction, while both Mg and Ca are known to be affected by sorption (Pogge von Strandmann et al., 2012; Tipper et al., 2021), and the exchangeable Li/Si, Mg/Si and Ca/Si ratios support the reliable extraction of an exchangeable fraction, and are also different from the dissolved fraction (Liu et al., 2022; Pogge von Strandmann et al., 2022). The oxide/oxyhydroxide phase Fe/Si ratios and clay Li/Si ratios also suggest that the sequential leaching methods are generally efficient at preferentially attacking the target phases, allowing us to draw useful conclusions from their Li isotope compositions (Liu et al., 2022; Pogge von Strandmann et al., 2022). This conclusion is also supported by laboratory experiments of basalt weathering, where these leaching methods are able to mass balance the Li lost from solution into secondary phases (Pogge von Strandmann et al., 2019b; Pogge von Strandmann et al., 2022). Based on the assumption that each leach only accessed its intended fraction, a mass balance of Li in the various secondary phases can be constructed (Fig. 2). Since no sequential leach method is fully efficient, these are likely to be overestimates of the Li in each fraction, if other phases are also leached, and underestimates if a phase is not completely leached. In these suspended load samples, the residue after leaching, which is likely to predominantly consist of primary basalt grains, makes up ~97% of the total particulate Li. The exchangeable fraction comprises on average ~ 0.25%, the oxides ~0.5%, and the clays ~1.6% of the particulate Li. For the oxides, this proportion is considerably less than observed in Icelandic soils (10–25%), but we note that a direct comparison cannot be made because those soils were selected for their greater weathering extent and high oxide contents (Pogge von Strandmann et al., 2021c).

The exchangeable fraction exhibits a wide variation in δ^7Li_{exch} values from −0.3 to +24.1‰, similar to the variation shown in the dissolved load. While there is no co-variation between the river discharge and δ^7Li_{exch} values, nor any observable effect of TSS on δ^7Li_{exch} values (i.e. no apparent effect of surface area), there is a > 99% significant (Spearman Rank) correlation between discharge and $\Delta^7Li_{exch\text{-}diss}$ (Fig. 3a). At low discharge (< 10 m^3/s, i.e. long water-rock interaction times), the $\Delta^7Li_{exch\text{-}diss}$ values remain approximately constant at −11.3 ± 0.6‰, and generally, direct-runoff rivers (which tend to have lower discharge) have broadly constant $\Delta^7Li_{exch\text{-}diss}$ values. This value is indistinguishable from the fractionation between the dissolved and exchangeable Li observed in basaltic weathering experiments that reached steady-state (−12‰, Pogge von Strandmann et al., 2019b; −12.7 ± 1.7‰, Pogge von Strandmann et al., 2022).

The oxides tend to be isotopically lighter than the exchangeable fraction, with δ^7Li_{ox} values ranging from −9.7 to +7.0‰, and there is a weak co-variation between $\Delta^7Li_{ox\text{-}diss}$ and discharge (Fig. 3b, also 99% significant (Spearman Rank)), with glacial rivers again exhibiting more variability. The values of the clay leach are intermediate between the exchangeable and oxide values, with δ^7Li_{clay} values ranging from −5.7 to +14.6‰. In comparison, the bulk suspended load (i.e. digested unleached sample, Table S4) has a narrow range in δ^7Li values of 4.3 ± 1.1‰, matching the typical compositions of MORB and Icelandic basalts and ash (Elliott et al., 2006; Pogge von Strandmann et al., 2012; Pogge von Strandmann et al., 2021c; Ryan and Kyle, 2004; Verney-Carron et al., 2015).

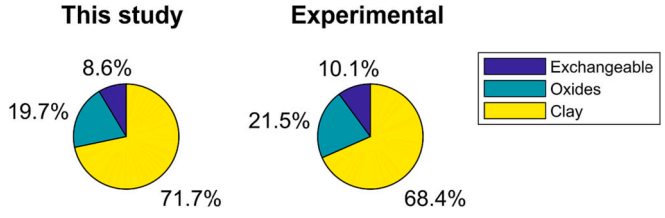

Fig. 2. Mass balance of the mean Li content in the different leached secondary phases (which comprise on average ~ 2.2% of the total suspended loads). For comparison, the experimental pie-chart represents the equivalent mass balance in basalt weathering experiments (Pogge von Strandmann et al., 2022).

In this study, given that there are some minor differences in δ^7Li values in Icelandic basalt (Pogge von Strandmann et al., 2012; Pogge von Strandmann et al., 2021c; Ryan and Kyle, 2004; Verney-Carron et al., 2015), we also normalise the clay δ^7Li values to their source lithologies. To do so, we calculate the δ^7Li values of the residue after leaching based on the bulk rock δ^7Li measurements and mass balance using the leach data. The composition of the residue is most likely to represent the initial primary basalt prior to weathering, but in any case the difference between the bulk rock and the residue δ^7Li values is ≤0.3‰, and is on average 0.02‰.

5. Discussion

5.1. General Li isotope behaviour in the dissolved load

Many global rivers exhibit a negative co-variation between dissolved δ^7Li values and Li/Na ratios, because Na is highly mobile and stays in solution, whereas Li is removed by secondary minerals, which also fractionate Li isotopes (Dellinger et al., 2015; Murphy et al., 2019). All basaltic rivers and soil pore waters, regardless of climate, show a similar trend in δ^7Li versus Li/Na space (Fig. 4), indicating that the fractionation factor in these weathering environments is fairly constant (Murphy et al., 2019; Pogge von Strandmann et al., 2017a). Icelandic basalt water-rock interaction experiments also show the same behaviour (Pogge von Strandmann et al., 2019b). For most mean basaltic samples, the fractionation pathway can be modelled with a Rayleigh-type relationship (i.e. a logarithmic one), with a fractionation factor α ~0.991–0.994 (Pogge von Strandmann et al., 2017a; Pogge von Strandmann et al., 2021c), and the new river samples from this study confirm this relationship (Fig. 4). In other words, the samples from this study exhibit fractionation behaviour typical of Icelandic weathering, and of basalt weathering in general.

5.2. Dissolved Li isotope behaviour with weathering rate

A key result of this study is that the dissolved Li isotope compositions correlate negatively with the chemical weathering rate (r^2 = 0.54; Fig. 5a), as in the study of Vigier et al. (2009). Considering the contributions to the weathering rate calculation, the δ^7Li values do not co-vary with TDS or the catchment area, but do correlate negatively with discharge (i.e. fluid flow per unit time; r^2 = 0.41; Fig. 5b) and runoff (i.e. discharge per unit of catchment area; r^2 = 0.47; Fig. 5c), with all relationships in Fig. 5 holding significance at the 99% confidence level (p < 0.01, Spearman Rank correlation). A priori, there is no clear reason why the addition of the catchment area to the relationship, to convert discharge to runoff, should still result in a correlation with δ^7Li values. However, in these rivers, there is a positive co-variation (r^2 = 0.56) between discharge and catchment area.

Thus, although not seasonally averaged, a similar trend to that of Zhang et al. (2022) is observed (Fig. 5b). Given that the discharge is the most fundamental parameter that co-varies with δ^7Li* values in our dataset, it follows that discharge is the factor controlling the dissolved δ^7Li* values. Thus, for low discharge (and low runoff), water-rock interaction time is longer, allowing more time for secondary mineral formation, driving [Li*] and Li*/Na* low, and $\delta^7Li^*_{diss}$ values high. In contrast, for high discharge, especially in weathering regimes such as Iceland which are dominantly kinetically-limited, water-rock interaction time is short, and therefore the dissolved δ^7Li values are closer to

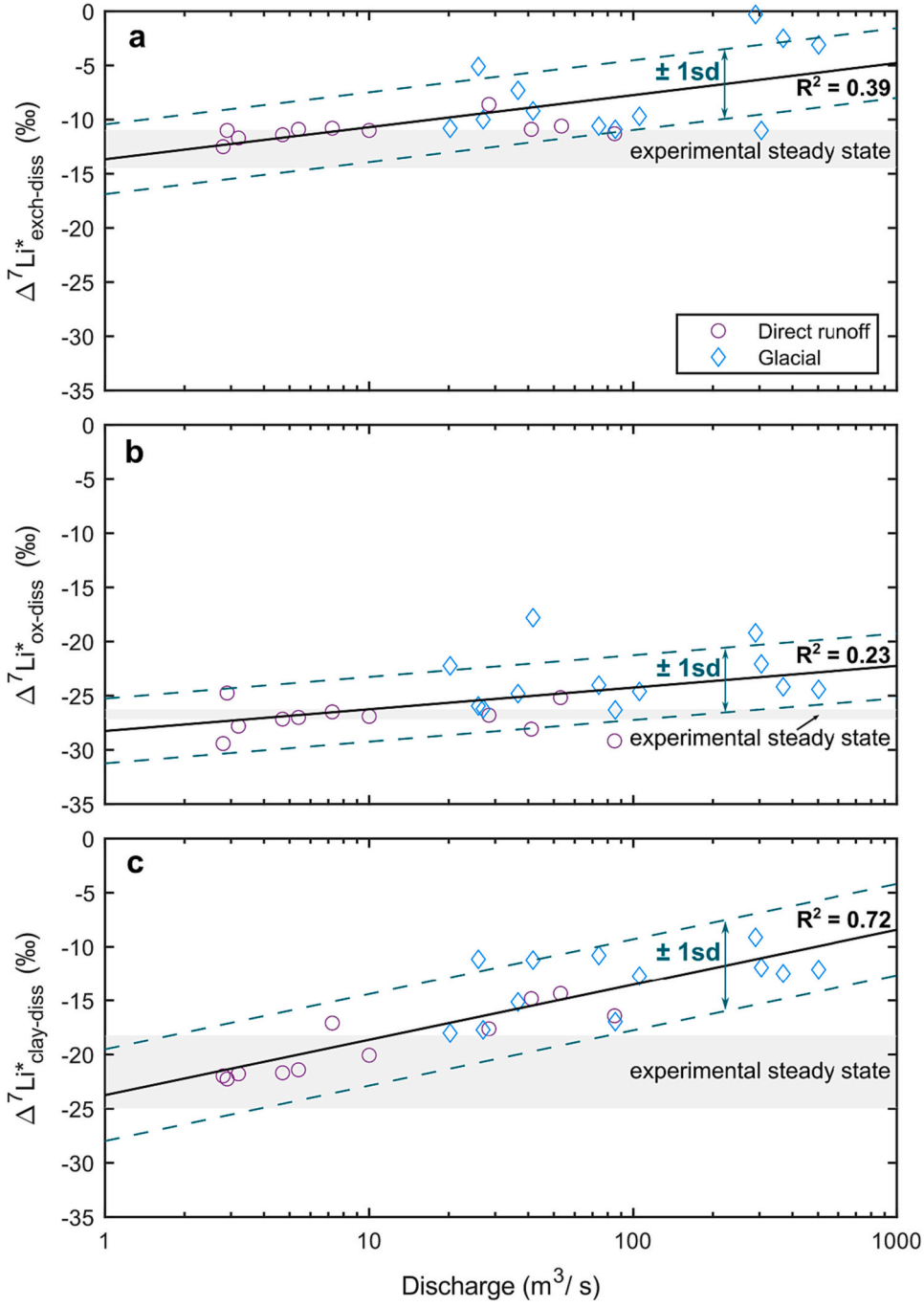

Fig. 3. Δ^7Li values showing the difference between the δ^7Li values of (a) the exchangeable fraction, (b) the oxide fraction, and (c) the clay fraction, and the corresponding dissolved load. The grey bars on each panel labelled 'experimental steady-state' represent the equilibrium fractionation observed in Icelandic basalt weathering experiments (Pogge von Strandmann et al., 2019b; Pogge von Strandmann et al., 2022). At low discharge (long water-rock interaction times), the observed fractionation is similar to experimental steady-state values. At high discharge (short water-rock interaction times), the magnitude of fractionation is less. The uncertainty on the values is smaller than the symbol sizes. All three correlations are >99% significant (Spearman Rank).

those of the host rock, and [Li*] and Li*/Na* are high (Zhang et al., 2022). We also note that the co-variation between δ^7Li_{diss} values and both discharge and runoff also results in a correlation between δ^7Li_{diss} and the weathering and erosion rates (Fig. 5a), and these correlations are therefore secondary. This scenario is discussed further in the context of the suspended load in Section 5.4.

5.3. Dissolved Li isotope behaviour with weathering intensity

The wide range in weathering intensity (W/D) of the samples in the present study allows us to test most of the relationship between δ^7Li_{diss} and W/D for a single lithology. In isolation, these Icelandic samples are consistent with the general boomerang shape, with the highest $\delta^7Li^*_{diss}$ values at medium weathering intensity, and lowest $\delta^7Li^*_{diss}$ values at low intensity. The $\delta^7Li^*_{diss}$ values also decrease as the W/D approaches a higher intensity, but they lie at the high end of the range previously reported for global rivers at those W/D values (Fig. 6).

In this study, we generally distinguish between the glacier-fed and direct-runoff rivers. However, we also examine the trends based on the more detailed river hydrology scheme of Oskarsdottir et al. (2011). The

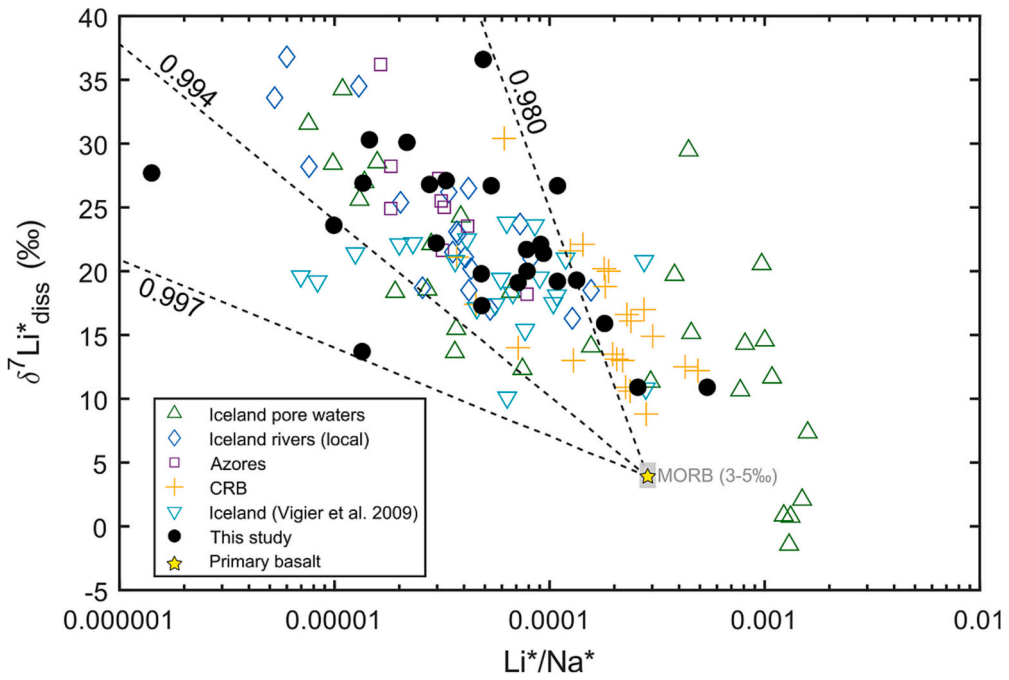

Fig. 4. Relationship of dissolved δ^7Li* values as a function of Li*/Na* ratios (* indicates precipitation-corrected). The dashed lines represent Rayleigh fractionation lines, with the numbers representing fractionation factors (α) (note the logarithmic x-axis). Also shown are comparative data from the Columbia River Basalts (CRB) (Liu et al., 2015), the Azores (Pogge von Strandmann et al., 2010), other Icelandic rivers (Pogge von Strandmann et al., 2006; Vigier et al., 2009), and Icelandic soil pore waters (Pogge von Strandmann et al., 2021c). The "local" Icelandic study focuses on a catchment in the west of Iceland (Pogge von Strandmann et al., 2006). The data from Vigier et al., 2009 are not precipitation-corrected, due to the lack of Cl^- data. The composition of primary basalt rock is shown with a grey box (Pogge von Strandmann et al., 2021c). The uncertainty on the δ^7Li* values is smaller than the symbol sizes.

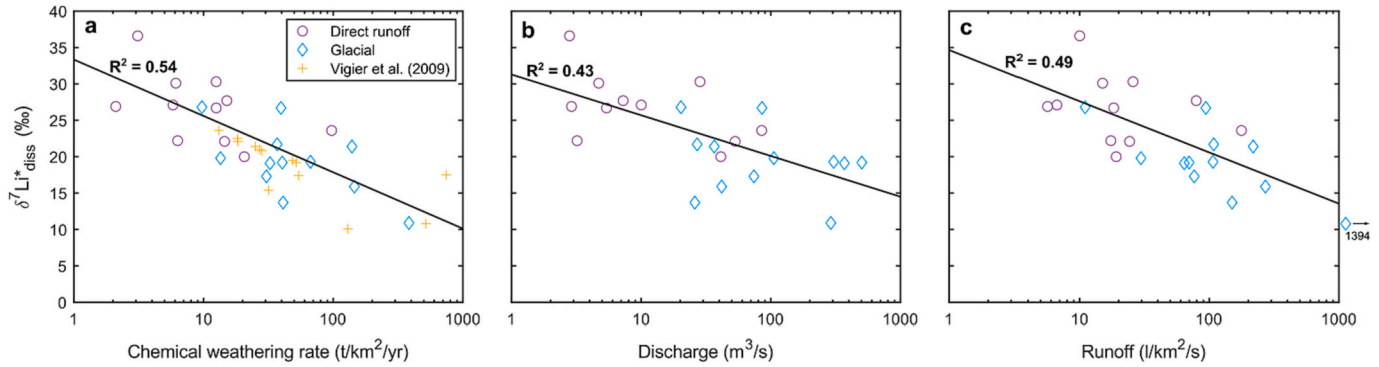

Fig. 5. Dissolved δ^7Li* values as a function of (a) chemical weathering rate (data from Vigier et al. (2009) also shown), (b) discharge, and (c) runoff. A logarithmic fit is shown because if the fit were linear, fractionation due to weathering could become negative at high rates (Pogge von Strandmann et al., 2021b; Vigier et al., 2009). All correlations are significant at the >99% confidence level (Spearman Rank correlation). The co-variation with discharge is considered primary, while that with the chemical weathering rate is most likely secondary (see text for details). The uncertainty on the analyses is smaller than the symbol sizes.

rivers with the lowest W/D values tend to be glacial rivers (average = 0.002), due to their high erosion rates, and they possess a low average δ^7Li*$_{diss}$ value of 17.3‰ (Fig. 6). In basaltic glacial rivers, pH depends on whether the water comes from surface melt (near-neutral pH) or basal melt (high pH). At high pH, primary mafic minerals become less undersaturated, and some clays become less supersaturated, while zeolites become more common (Stefansson and Gislason, 2001). Further, for eruptions under glaciers, hyaloclastite (glass-rich basalt) is common (Gíslason et al., 1996). Overall, sufficient secondary minerals still form in such systems to lead to fractionated Li isotope compositions. Medium weathering intensity rivers are dominated by direct-runoff rivers with soil storage, which have a higher average δ^7Li*$_{diss}$ value of 28.8‰ (Fig. 6). These results fit with our expectation, given that soil storage causes longer water-rock interaction times. Direct-runoff rivers that drain highlands with little soil storage also have medium weathering intensities, but have somewhat lower average δ^7Li*$_{diss}$ values of 21.2‰. The higher intensity weathering regimes, which in Iceland do not extend to the highest values observed in global compilations (Fig. 6), are largely groundwater-fed rivers, with some additional direct-runoff river samples. The groundwater-fed rivers have an average δ^7Li*$_{diss}$ value of 25.2‰. Low-temperature groundwaters in Iceland have similar δ^7Li values of around 23‰ (Pogge von Strandmann et al., 2006; Pogge von Strandmann et al., 2016). Groundwaters effectively reflect systems with (very) low erosion rates and a relatively supply-limited weathering regime. However, the δ^7Li values are not low enough to indicate extensive dissolution of pre-existing secondary minerals, as observed in highly supply-limited regimes (Dellinger et al., 2015).

In summary, while the δ^7Li versus W/D relationship for Icelandic basaltic rivers follows the broad patterns of global rivers (Dellinger et al., 2015), the riverine δ^7Li values never drop to the very low values

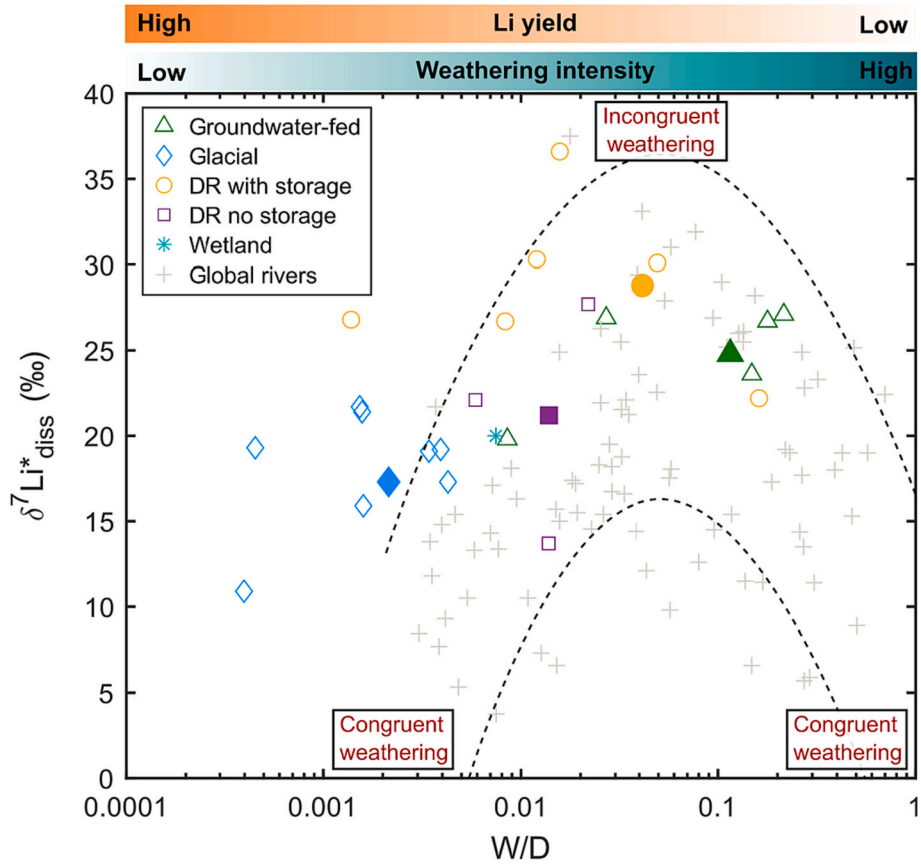

Fig. 6. Dissolved δ^7Li^* values as a function of the weathering intensity (W/D, where W = weathering, D = denudation). The rivers from this Icelandic study are categorised using a different weathering scheme (Oskarsdottir et al., 2011) from the other diagrams, and the solid symbols for each category represent that category's average. Global river compilations (Dellinger et al., 2015; Pogge von Strandmann et al., 2021d) are shown as grey crosses. The dashed lines represent the "original" boomerang of Dellinger et al. (2015). DR = direct-runoff.

previously observed at low or approaching high W/D ratios. This finding appears to be a particular feature of the rapid secondary mineral formation during basaltic weathering. During the basalt weathering experiments described in the Introduction, solution δ^7Li values immediately (within <1 day) increase (Pogge von Strandmann et al., 2019b; Pogge von Strandmann et al., 2022). In other words, it appears that for basalt weathering under kinetic-limitation (low W/D), there is nevertheless always a fairly large degree of secondary mineral formation (in those experiments the secondary minerals are thought to be smectite, allophane and oxides such as ferrihydrite and goethite). This scenario contrasts with the weathering of continental crust lithologies, where secondary mineral formation tends to be slower, and hence riverine δ^7Li values in such highly kinetically-limited weathering regimes can be very close to the values of the host rock (Dellinger et al., 2015; Pogge von Strandmann et al., 2021a). For basaltic weathering systems at higher W/D, any leaching of secondary minerals would also be expected to yield relatively high δ^7Li values, because these minerals are relatively isotopically heavy (see Section 5.4)).

Aside from this, there are similarities in the general weathering intensity behaviour in these basaltic rivers compared to global rivers when Li weathering yields (amount per unit area and unit time) are considered. In global compilations, high W/D rivers have lower Li yields (Pogge von Strandmann et al., 2020; Pogge von Strandmann et al., 2021d), because clays are more stable than primary minerals, whereas the high erosion rates and minimal clay formation under low W/D conditions promote dissolution and Li retention in solution. The same relationship is seen in this study (Fig. 7), and although none of these basaltic rivers extend to the very highest of weathering intensities (W/D $\geq$ 0.5), expanding the line of best fit for our data suggests a variance in Li yield of more than an order of magnitude between low intensity regimes (W/D $\leq$ 0.01) and high intensity regimes (W/D $\geq$ 0.2). This further supports the assumption that high W/D environments have a very limited impact on global seawater budgets in the present-day or in the past, due to the much lower Li yields (Pogge von Strandmann et al., 2021d).

Overall, the above findings indicate a plausible mechanism by which different weathering processes control the basaltic version of the "boomerang" plot. For the original boomerang, that was based on a global compilation, the effects of different lithologies were thought to be excluded by plotting $\Delta^7Li_{dissolved\text{-}host\ rock}$ rather than simply δ^7Li_{diss} (Dellinger et al., 2015). Here, by examining the relationship between W/D and δ^7Li_{diss} values within a single lithology, we show that the boomerang shape still exists, but that lithology exerts an influence beyond simply changing the $\delta^7Li_{host\ rock}$ values. Instead, lithology-specific dissolution rates and secondary mineral formation rates also appear to have an effect. In particular, in the case of basaltic weathering, it seems that very low δ^7Li_{diss} values cannot be generated, even at very low W/D ratios (Fig. 6), due to the very rapid secondary mineral formation (in Iceland likely initially allophane and ferrihydrite, followed by smectite; Pogge von Strandmann et al., 2021c; Stefansson and Gislason, 2001).

An interesting consequence of this specific feature of basalt dissolution may be found in the geological record, for example during Oceanic Anoxic Events (OAEs), which are thought to have been triggered by the eruption of (typically basaltic) large igneous provinces. The negative marine Li isotope excursions observed during both OAE 1a and 2 have been interpreted in terms of the rapid weathering of very fresh continental basalt following its sudden emplacement (Lechler et al.,

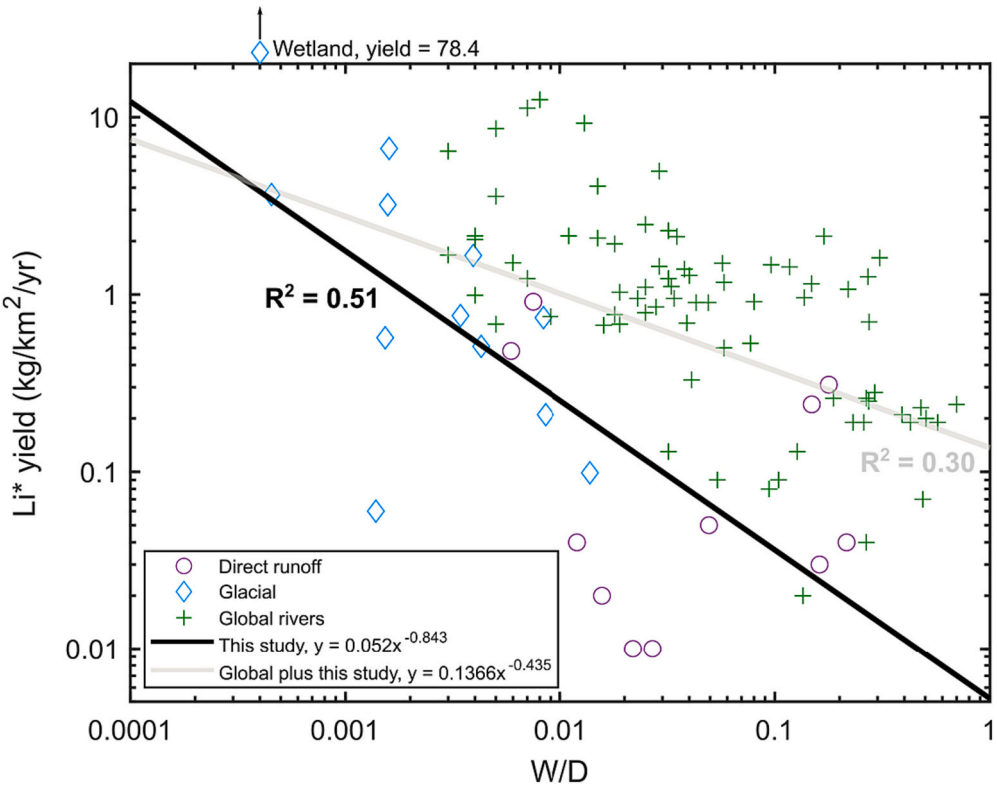

Fig. 7. Precipitation-corrected river dissolved Li yields as a function of the weathering intensity (W/D, where W = weathering, D = denudation). Global rivers (Dellinger et al., 2015; Pogge von Strandmann et al., 2021d) are also shown as green crosses. (For interpretation of the references to colour in this figure legend, the reader is referred to the web version of this article.)

2015; Pogge von Strandmann et al., 2013). However, the data in this study, together with basalt weathering experiments (Pogge von Strandmann et al., 2019b; Pogge von Strandmann et al., 2022), suggest that basaltic weathering may instead rapidly drive riverine δ^7Li values higher. As such, the negative marine Li isotope excursions during OAEs may actually reflect enhanced weathering and erosion of continental crust-like material driven by the CO_2 release, rather than being dominated by basalt weathering. Such a hypothesis of continental crustal weathering has also been invoked to explain a similar marine Li isotope excursion during the Palaeocene-Eocene Thermal Maximum (Pogge von Strandmann et al., 2021d), for which there is no evidence of a large subaerial eruption of basalt, so this hypothesis may be more widely applicable.

5.4. Lithium and Li isotopes in the suspended load

5.4.1. Exchangeable fraction

Together, the exchangeable leach results from this study and basaltic weathering experiments (Pogge von Strandmann et al., 2019b; Pogge von Strandmann et al., 2022) imply that, for basaltic weathering reactions that have sufficient time to reach steady-state (i.e. constant dissolved Li isotope ratios, likely representing dynamic equilibrium), the isotope fractionation factor of the exchangeable fraction is constant. In contrast, at higher discharge, the $\Delta^7Li_{exch\text{-}diss}$ values increase and are close to zero at the highest discharge values (Fig. 3a). It therefore appears that achieving full steady-state (likely dynamic equilibrium) fractionation, as determined by experiments that were in steady-state for several months, takes time, with more rapid reactions resulting in less fractionation between the exchangeable and dissolved loads. The effect of reaction time may also explain the range in $\Delta^7Li_{exch\text{-}diss}$ values reported in other experimental studies (0–12‰; Chan and Hein, 2007; Hindshaw et al., 2019; Pogge von Strandmann et al., 2020; Wimpenny et al., 2015). Finally, we also note that there are no co-variations between the $\Delta^7Li_{exch\text{-}diss}$ values and other parameters that might be expected to control weathering reactions, such as temperature or pH.

5.4.2. Oxide fraction

When considering the oxide fraction as a percentage of only the secondary phases (i.e. those leached), the oxides make up approximately 15–30% of the Li budget (Fig. 2). This proportion co-varies with pH in an almost identical manner to that seen in basalt weathering experiments (Fig. 8a; Pogge von Strandmann et al., 2022). These findings suggest that there is a strong pH control on the removal of Li into oxides/oxyhydroxides. This trend is broadly similar to the supersaturation of such oxide minerals (e.g. hematite and goethite; Fig. 8b), which suggests that at least part of this co-variation may be due to the increased precipitation of oxides as a function of increasing pH, rather than just pH-dependent Li partitioning.

Overall, the Li isotope fractionation between the oxide and dissolved fractions remains relatively constant, at $\Delta^7Li_{ox\text{-}diss} = -25.0 \pm 3.0$‰ (Fig. 3b). However, in a similar manner to the exchangeable fraction, the oxide/oxyhydroxide fraction also exhibits a $\Delta^7Li_{ox\text{-}diss}$ relationship with the discharge. The fractionation at low discharge ($\leq$10 m^3/s) is -27 ± 1.4‰, in good agreement with observations from basaltic weathering experiments that have reached steady-state (-26.7 ± 0.4‰; Pogge von Strandmann et al., 2022). At higher discharge, the magnitude of fractionation is less, but even at the highest discharge (>200 m^3/s), the fractionation is still large, with $\Delta^7Li_{ox\text{-}diss} = -21 \pm 2.2$‰ (Fig. 3b). The rate of oxide and oxyhydroxide formation is likely faster than the clay formation rate (Snæbjörnsdóttir et al., 2018; Stefansson and Gislason, 2001), but it is slower than the response time of the exchangeable fraction, which may have an impact on the "boomerang", as discussed below.

5.4.3. Clay fraction

Using the δ^7Li values of the clay leach compared to the source

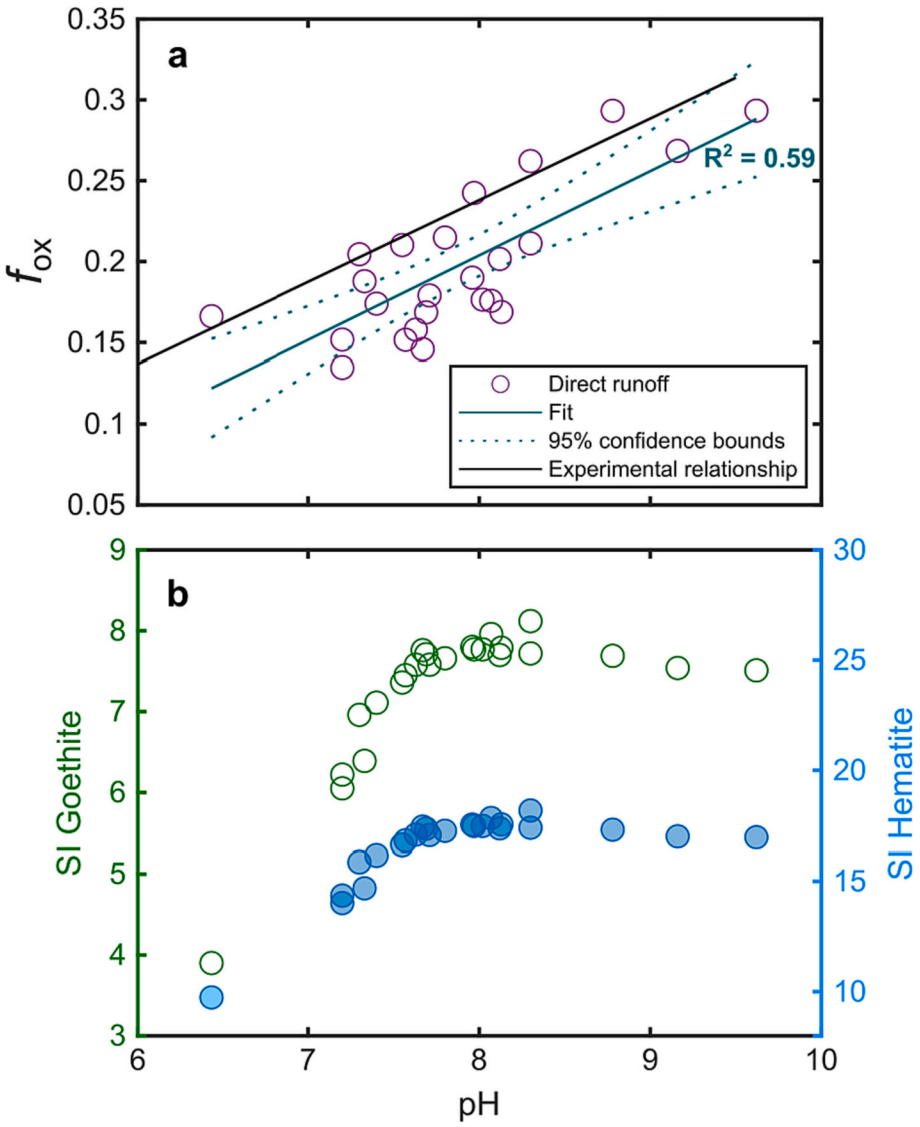

Fig. 8. (a) Fractional contribution of oxide-bound Li to the total leached (exchangeable, oxide, clay) fraction in the Icelandic river sediments, as a function of pH. The blue line with 95% confidence bounds is the trend line of the river sediment data, while the black line is the relationship observed in basalt weathering experiments (Pogge von Strandmann et al., 2022). (b) Calculated saturation indices of goethite (green circles) and hematite (blue filled circles) in the Icelandic river samples. (For interpretation of the references to colour in this figure legend, the reader is referred to the web version of this article.)

composition, the $\Delta^7Li_{clay\text{-}source}$ clearly does not follow the multi-lithological trend of Dellinger et al. (2017) (Fig. 9b). Generally, the Icelandic clays are slightly isotopically heavier than the residue (on average by ~2‰), regardless of whether the weathering regime is of low or approaching relatively (for Iceland) high intensity. At medium W/D values, $\Delta^7Li_{clay\text{-}source}$ values are highest (up to ~10‰), so this pattern appears more similar to the boomerang shape exhibited by dissolved δ^7Li values as a function of W/D, with highest values at medium W/D, and lower values at low and higher W/D.

Such a relationship of $\Delta^7Li_{clay\text{-}source}$ values with the weathering intensity (Fig. 9b), and the fact that the clays are isotopically heavier than the initial rock, suggests that the clays are precipitating from isotopically heavy solutions, as also, for example, observed during the alteration of the oceanic crust (e.g. Chan et al., 1992). From a mass balance perspective, an equilibrium fractionation scenario is not possible, because secondary minerals separated from solutions by a constant fractionation factor can never become isotopically heavier than the initial rock, but is possible with a kinetic fractionation-type relationship. Kinetic fractionation (mathematically represented by a Rayleigh fractionation relationship) for Li isotopes has been repeatedly documented for both experimental and natural basaltic weathering (Li et al., 2021; Liu et al., 2015; Pogge von Strandmann et al., 2017a; Pogge von Strandmann et al., 2010; Pogge von Strandmann et al., 2012; Pogge von Strandmann et al., 2021c; Pogge von Strandmann et al., 2019b; Pogge von Strandmann et al., 2022; Vigier et al., 2009), as well as for the weathering of other rock types (e.g. Kisakurek et al., 2004; Maffre et al., 2020; Pogge von Strandmann et al., 2019a; Wanner et al., 2014; Zhang et al., 2021). In effect, for basalt at least, this finding suggests that the uptake of Li from solution by secondary minerals can, initially at least, be faster than the supply by dissolution, resulting in a nominally "closed" system. In experiments this results in solution [Li] decreasing by an order of magnitude (Pogge von Strandmann et al., 2019b; Pogge von Strandmann et al., 2022).

However, the case here in Iceland appears slightly more complex than this simple scenario, since the fractionation between clay and solution is also not constant. Instead, like the other leached fractions of the suspended load, the $\Delta^7Li_{clay\text{-}diss}$ values also correlate with discharge rates (Fig. 3c). The $\Delta^7Li_{clay\text{-}diss}$ values are greatest in low-discharge regimes, with values reaching −22‰, and are smallest in high-discharge regimes, with values reaching −9‰. As with the other two leached

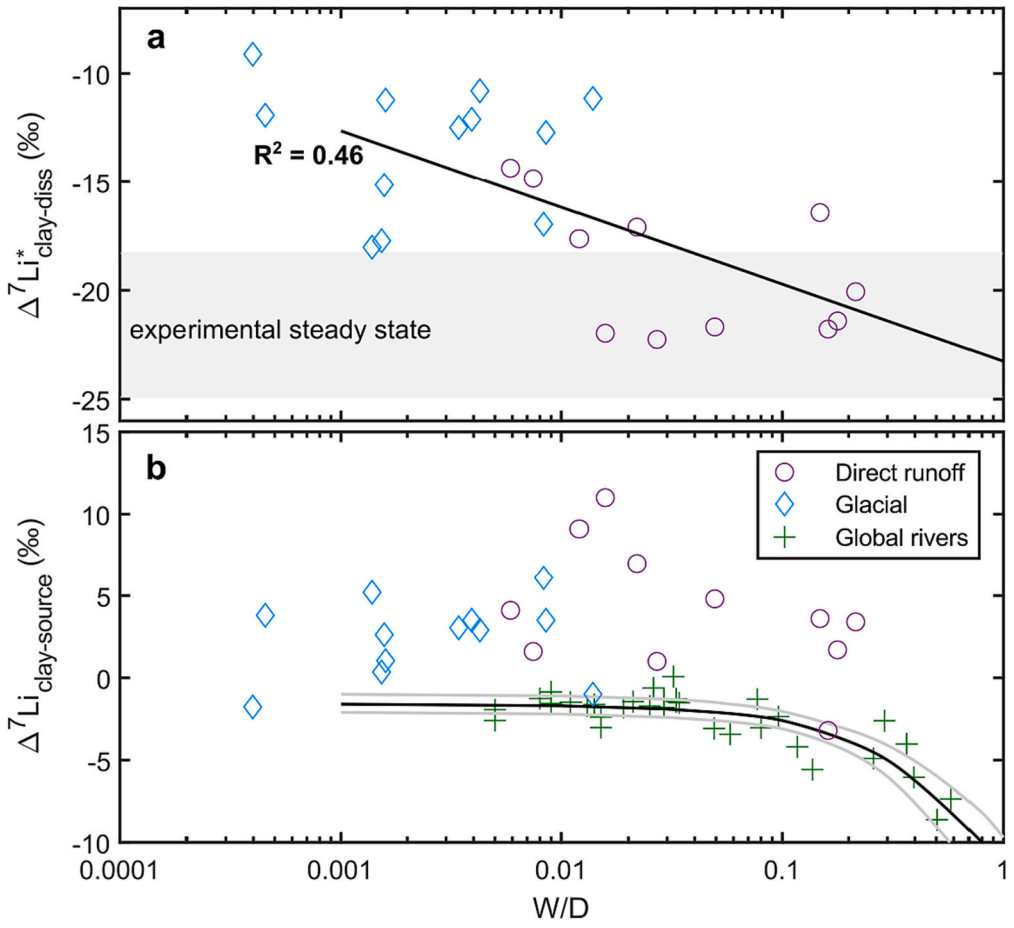

Fig. 9. (a) Relationship between the weathering intensity (W/D, where W = weathering, D = denudation) and the difference between the δ^7Li values of the clay fraction and the dissolved fraction. The grey bar labelled 'experimental steady-state' is the equilibrium fractionation observed in basalt weathering experiments (Pogge von Strandmann et al., 2019b; Pogge von Strandmann et al., 2022). (b) Relationship between weathering intensity (W/D) and the difference between the δ^7Li values of the clay fraction and the primary source rock (here, the calculated $\delta^7Li_{residue}$ after leaching; see text for details). The green crosses represent fine-grained data (<0.6 μm size fraction) from a global multi-lithological compilation, while the black line and its error margins represent their trend (Dellinger et al., 2017). Our Icelandic basalt clay Li isotope data are more similar to the boomerang-shaped relationship of the dissolved load Li isotopes than to the clay relationship seen by Dellinger et al. (2017). (For interpretation of the references to colour in this figure legend, the reader is referred to the web version of this article.)

fractions, the fractionation at the lowest discharge rates is similar to the fractionation observed in basalt weathering experiments that reached steady-state (−22‰; Pogge von Strandmann et al., 2019b; Pogge von Strandmann et al., 2022). It therefore appears that, if the reaction time is minimal (i.e. high discharge), then full equilibrium fractionation is not reached, and this finding applies to all of the different suspended load phases. The observed fractionation factor should be a mixture of the rapidly reacting interlayer sites (although to an extent these will have been removed by the exchangeable leach), and the more slowly reacting structural layer incorporation. This situation leads to a relationship of $\Delta^7Li_{clay\text{-}diss}$ with the weathering intensity that is different from that of $\Delta^7Li_{clay\text{-}source}$: at low W/D in glacier-fed rivers, there is least isotope fractionation between the clay and dissolved loads, and at moderately high W/D (when discharge rates are low), the fractionation is greatest (Fig. 9a).

Hence, the (neoformed) clay fraction gains its Li from the isotopically heavy weathering solutions. As for the solutions (Fig. 4), we assume that the variable Δ^7Li values are due to variable uptake with a constant fractionation factor α, rather that due to a variable α value. This makes sense, given that 1) different secondary minerals within the oxides or clays do not appear to have appreciably different fractionation factors (Hindshaw et al., 2019; Pogge von Strandmann et al., 2022), and 2) in any case, the dominant secondary minerals do not vary particularly in Iceland (Pogge von Strandmann et al., 2021c). From this we can construct a kinetic fractionation pathway (mathematically the same as Rayleigh fractionation) for secondary minerals that formed from supersaturated solutions, with a fresh basalt starting composition (Fig. 10). These calculations factor in the varying proportions that the bulk secondary minerals are made up by the different secondary phases, with their different fractionation factors (α).

With these fractionation factors, the river waters follow a broadly simple fractionation pathway, reaching the $\delta^7Li^*_{diss}$ values observed here between ~40 and 80% removal of Li from solution. The bulk secondary minerals (i.e. those taking Li out of solution), calculated from the fractionation factors and proportions that the different phases make up (Fig. 2), reach the δ^7Li value of the initial basalt once ~60% of Li has been removed from solution, and finally reach their highest observed δ^7Li values (of 14.7‰) at ~78% Li removal from solution. A Rayleigh relationship in principle also allows the calculation of the accumulated secondary phases. However, the δ^7Li of such an accumulation also would not have isotope ratios higher than the initial basalt. Hence, in this case at least, the total accumulated secondary minerals are not being sampled, almost certainly because the earlier, initial, secondary minerals (at higher numbers of f_{Li}) have already been transported away, and hence each particle no longer contains an entire "history" of secondary mineral formation. It is also possible that the leaching method is preferentially attacking the later-formed phases.

The overall point of these calculations is that, for basalt weathering

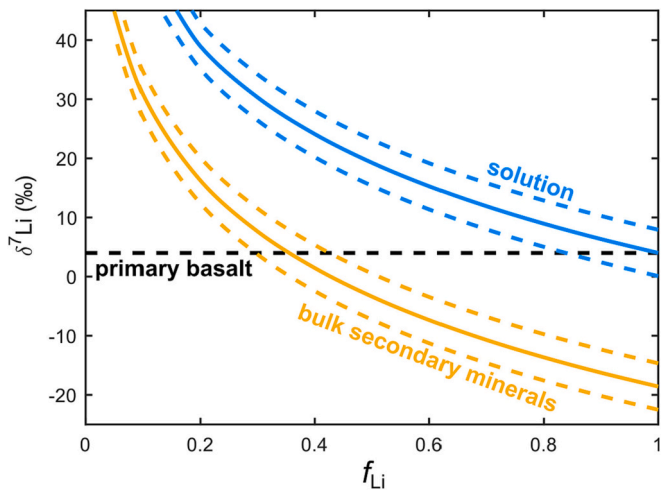

Fig. 10. Modelled solution and bulk secondary mineral δ^7Li values as a function of the fraction of Li remaining in solution (f_{Li}) using a kinetic fractionation model, when factoring in the variable proportions of the different secondary phases (exchangeable, oxide and clay) and the fractionation observed in this study (e.g. average α_{exch} = 0.9875; average α_{ox} = 0.973; average α_{clay} = 0.9782). The evolution of values shows that secondary minerals can have δ^7Li values higher than the initial rock if sufficient Li is removed from solution.

(or any other weathering where Rayleigh fractionation applies), secondary minerals are only isotopically lighter than the original basalt under certain conditions. Instead, for scenarios where a relatively high amount of Li is removed from solution, as generally observed during basalt weathering (Pogge von Strandmann et al., 2017a; Pogge von Strandmann et al., 2021c), the secondary minerals can be isotopically heavier than the original rock, because the dissolved load from which they form becomes increasingly isotopically heavy. This is also observed during clay formation from ocean basalts (e.g. Chan et al., 1992).

Overall, this scenario is interesting because it opens up the possibility for clay δ^7Li values to respond sensitively to the weathering regimes at all values of W/D, which would strengthen the use of detrital or continental clays as a weathering archive (Bastian et al., 2017; Li et al., 2016; Pogge von Strandmann et al., 2017b; Pogge von Strandmann et al., 2021d; Ramos et al., 2022; Wei et al., 2020; Yin et al., 2023). Notably, the highest clay δ^7Li values may be expected for intermediate W/D regimes, broadly similar to the pattern observed in the dissolved load. However, given that the fractionation between clay and solution does not appear to be constant (depending instead on the discharge and the associated weathering regime), it seems that quantitatively reconstructing solution δ^7Li values from clays (e.g. those separated by leaching or density settling, rather than only sieving) will be a complex task.

Developing clays as an archive of δ^7Li values will therefore require more work to establish whether the behaviour observed here for basalt weathering also occurs during weathering of other lithologies, given that the current curve reported by Dellinger et al. (2017) consists of a trend where samples from one region tend to cluster in one part of the W/D trend. If the same observation does indeed apply to other lithologies, it will help confirm one potential cause for the observed step-wise increase in seawater δ^7Li values in the early Palaeozoic (Kalderon-Asael et al., 2021). In that study, it was hypothesised that a decrease in oceanic Si concentrations led to a slow-down in reverse weathering rates (i.e. authigenic clay formation in the oceans), which would have caused longer sediment-water interaction times, and is modelled to have increased Δ^7Li values between sediment and seawater. Our direct observations from Iceland appear to confirm such a time-dependent control on Δ^7Li values as seen in those model results.

Overall, the combined analyses of solid and dissolved phases reveal the entire process of Li isotope fractionation in rivers. At high discharge (low W/D), water-rock interaction times are short, which enables relatively little clay formation, and therefore high Li yields. Hence, apparent Li isotope fractionation between secondary clays and the dissolved load is limited meaning there is little isotopic difference between the initial rock and the dissolved load, and thus dissolved δ^7Li values are also low. At lower discharge rates (medium W/D), water-rock interaction times are longer, enabling more clay formation, while there is also greater apparent isotope fractionation between clays (and other secondary phases) and the dissolved load. This scenario causes the dissolved load to evolve towards high δ^7Li values, which in turn gives the next parcel of secondary minerals that form higher δ^7Li values than the previous one (Fig. 10).

6. Conclusions

This is the first study to investigate the interaction between river discharge, weathering intensity, and Li isotope compositions for both the dissolved and solid loads in a mono-lithological environment. The observations for the dissolved load generally confirm observations from global multi-lithological compilations, namely that δ^7Li_{diss} values decrease as discharge increases (due to shorter water-rock interaction times), and that there is a "boomerang" shaped relationship between weathering intensity (W/D) and δ^7Li_{diss} values. However, δ^7Li_{diss} values in the basaltic environment never reach the very low values observed in the global compilation for low W/D regimes, due to the apparently very rapid secondary mineral formation that occurs during basaltic weathering. This finding suggests that there are lithological effects on the relationship between W/D and δ^7Li_{diss} values that transcend the slightly different δ^7Li values of the initial rock and may be controlled by the precipitation rates of the different secondary minerals that form during weathering of different lithologies.

The Δ^7Li difference between sequentially-leached phases of the suspended load (exchangeable, oxide and clay) and the corresponding solutions generally agree with basaltic experimental values, but only at lower discharge rates (long water-rock interaction times), when steady-state has been reached. At high discharge, the Δ^7Li values of all three phases approaches 0, suggesting that fractionation is reduced when water-rock interaction time is low. Therefore, Δ^7Li values between the clay fraction and the source are a function of W/D, with the relationship differing from previous global compilations. The clay δ^7Li values more closely follow the boomerang shape of the dissolved load, rather than only being sensitive to weathering intensity in high W/D regimes, as previously thought. This relationship implies that the clays (and other secondary phases) observed here obtained their Li directly from an already isotopically-heavy dissolved load.

Similar observations need to be conducted in other mono-lithological terrains, but we can already point to potential consequences for the use of Li isotopes as a tracer of palaeo-weathering. For example, 1) rapid basaltic clay formation, and consequently high δ^7Li_{diss} values, suggest that negative seawater δ^7Li excursions observed during nominal basaltic eruption events (such as OAEs) may have arisen from accelerated weathering and erosion of continental crustal lithologies due to CO_2 release, rather than simply indicating the direct weathering of freshly-exhumed basalt; 2) the smaller $\Delta^7Li_{clay\text{-}dissolved}$ linked to short water-rock interaction times confirms that less Li isotope fractionation would occur during accelerated reverse weathering, in turn supporting the hypothesis that high reverse weathering may have been a cause of low seawater δ^7Li values during the Precambrian; and 3) the fractionation between clays and the dissolved load is not constant, but depends on discharge (water-rock interaction time), which complicates the interpretation of detrital δ^7Li records, but may also open an interesting avenue for reconstructing hydrological changes.

Declaration of Competing Interest

The authors declare that they have no known competing financial

interests or personal relationships that could have appeared to influence the work reported in this paper.

Data availability

The data tables for this study are available at the following DOI: https://doi.org/10.5522/04/23274680

Acknowledgements

We thank Gary Tarbuck, Carolin Berg, and Regina Walter for their help during elemental concentration measurements. UCL is thanked for supporting the MSci of LC and funding the associated measurements. Other analyses and PPvS and AJK were funded by ERC grant 682760 CONTROLPASTCO2. Analytical equipment was funded by the Carl Zeiss + German Scholars Organisation programme GSO/CZS 36, and DFG grant INST 247/1095-1 to PPvS. DJW was supported by a Natural Environment Research Council independent research fellowship (NE/T011440/1). For the purpose of open access, the author has applied a 'Creative Commons Attribution (CC BY) licence' to any Author Accepted Manuscript version arising.

Appendix A. Supplementary data

Supplementary data to this article can be found online at https://doi.org/10.1016/j.chemgeo.2023.121801.

References

Bastian, L., Revel, M., Bayon, G., Dufour, A., Vigier, N., 2017. Abrupt response of chemical weathering to Late Quaternary hydroclimate changes in Northeast Africa. Sci. Rep. 7, 44231.
Berner, R.A., 2003. The long-term carbon cycle, fossil fuels and atmospheric composition. Nature 426, 323–326.
Berner, R.A., Lasaga, A.C., Garrels, R.M., 1983. The carbonate-silicate geochemical cycle and its effect on atmospheric carbon-dioxide over the past 100 million years. Am. J. Sci. 283, 641–683.
Bouchez, J., von Blanckenburg, F., Schuessler, J.A., 2013. Modeling novel stable isotope ratios in the weathering zone. Am. J. Sci. 313.
Brant, C., Coogan, L.A., Gillis, K.M., Seyfried, W.E., Pester, N.J., Spence, J., 2012. Lithium and Li-isotopes in young altered upper oceanic crust from the East Pacific Rise. Geochim. Cosmochim. Acta 96, 272–293.
Caves Rugenstein, J.K., Ibarra, D.E., von Blanckenburg, F., 2019. Neogene cooling driven by land surface reactivity rather than increased weathering fluxes. Nature 571, 99–102.
Chan, L.H., Hein, J.R., 2007. Lithium contents and isotopic compositions of ferromanganese deposites from the global ocean. Deep-Sea Res. 54, 1147–1162.
Chan, L.H., Edmond, J.M., Thompson, G., Gillis, K., 1992. Lithium isotopic composition of submarine basalts: implications for the lithium cycle in the oceans. Earth Planet. Sci. Lett. 108, 151–160.
Clergue, C., Dellinger, M., Buss, H.L., Gaillardet, J., Benedetti, M.F., Dessert, C., 2015. Influence of atmospheric deposits and secondary minerals on Li isotopes budget in a highly weathered catchment, Guadeloupe (Lesser Antilles). Chem. Geol. 414, 28–41.
Dellinger, M., Gaillardet, J., Bouchez, J., Calmels, D., Louvat, P., Dosseto, A., Gorge, C., Alanoca, L., Maurice, L., 2015. Riverine Li isotope fractionation in the Amazon River basin controlled by the weathering regimes. Geochim. Cosmochim. Acta 164, 71–93.
Dellinger, M., Bouchez, J., Gaillardet, J., Faure, L., Moureau, J., 2017. Tracing weathering regimes using the lithium isotope composition of detrital sediments. Geology 45, 411–414.
Dosseto, A., Vigier, N., Joannes-Boyau, R., Moffat, I., Singh, T., Srivastava, P., 2015. Rapid response of silicate weathering rates to climate change in the Himalaya. GPL 1, 10–19.
Eiriksdottir, E.S., Gislason, S.R., Oelkers, E.H., 2013. Does temperature or runoff control the feedback between chemical denudation and climate? Insights from NE Iceland. Geochim. Cosmochim. Acta 107, 65–81.
Elliott, T., Thomas, A., Jeffcoate, A., Niu, Y.L., 2006. Lithium isotope evidence for subduction-enriched mantle in the source of mid-ocean-ridge basalts. Nature 443, 565–568.
Gislason, S.R., Eugster, H.P., 1987. Meteoric water-basalt interactions. II: a field study in N.E. Iceland. Geochim. Cosmochim. Acta 51, 2841–2855.
Gíslason, S.R., Arnorsson, S., Armannsson, H., 1996. Chemical weathering of basalt in Southwest Iceland: effects of runoff, age of rocks and vegetative/glacial cover. Am. J. Sci. 296, 837–907.
Golla, J.K., Bouchez, J., Kuessner, M.L., Rempe, D.M., Druhan, J.L., 2022. Subsurface weathering signatures in stream chemistry during an intense storm. Earth Planet. Sci. Lett. 595, 117773.
Grimm, C., Martinez, R.E., Pokrovsky, O.S., Benning, L.G., Oelkers, E.H., 2019. Enhancement of cyanobacterial growth by riverine particulate material. Chem. Geol. 525, 143–167.
Hedges, J.I., Keil, R.G., 1995. Sedimentary organic matter preservation: an assessment and speculative synthesis. Mar. Chem. 49, 81–115.
Hindshaw, R.S., Bourdon, B., Pogge von Strandmann, P.A.E., Vigier, N., Burton, K.W., 2013. The stable calcium isotopic composition of rivers draining basaltic catchments in Iceland. Earth Planet. Sci. Lett. 374, 173–184.
Hindshaw, R.S., Tosca, R., Gout, T.L., Farnan, I., Tosca, N.J., Tipper, E.T., 2019. Experimental constraints on Li isotope fractionation during clay formation. Geochim. Cosmochim. Acta 250, 219–237.
Huh, Y., Chan, L.H., Edmond, J.M., 2001. Lithium isotopes as a probe of weathering processes: Orinoco River. Earth Planet. Sci. Lett. 194, 189–199.
Jeffcoate, A.B., Elliott, T., Thomas, A., Bouman, C., 2004. Precise, small sample size determinations of lithium isotopic compositions of geological reference materials and modern seawater by MC-ICP-MS. Geostand. Geoanal. Res. 28, 161–172.
Jones, M.T., Gislason, S.R., Burton, K.W., Pearce, C.R., Mavromatis, V., Pogge von Strandmann, P.A.E., Oelkers, E.H., 2014. Quantifying the impact of riverine particulate dissolution in seawater on ocean chemistry. Earth Planet. Sci. Lett. 395, 91–100.
Kalderon-Asael, B., Katchinoff, J.A.R., Planavsky, N.J., Hood, A.V.S., Dellinger, M., Bellefroid, E.J., Jones, D.S., Hofmann, A., Ossa Ossa, F., Macdonald, F.A., Wang, C., Isson, T.T., Murphy, J.G., Higgins, J.A., West, A.J., Wallace, M.W., Asael, D., Pogge von Strandmann, P.A.E., 2021. A lithium-isotope perspective on the evolution of carbon and silicon cycles. Nature 595, 394–398.
Kennedy, M.J., Wagner, T., 2011. Clay mineral continental amplifier for marine carbon sequestration in a greenhouse ocean. Proc. Natl. Acad. Sci. 108, 9776–9781.
Kisakurek, B., Widdowson, M., James, R.H., 2004. Behaviour of Li isotopes during continental weathering: the Bidar laterite profile, India. Chem. Geol. 212, 27–44.
Kisakürek, B., James, R.H., Harris, N.B.W., 2005. Li and δ^7Li in Himalayan rivers: proxies for silicate weathering? Earth Planet. Sci. Lett. 237, 387–401.
Krause, A.J., Sluijs, A., van der Ploeg, R., Lenton, T.M., Pogge von Strandmann, P.A.E., 2023. Enhanced clay formation key in sustaining the Middle Eocene Climatic Optimum. Nat. Geosci. 16, 730–738.
Lalonde, K., Mucci, A., Ouellet, A., Gelinas, Y., 2012. Preservation of organic matter in sediments promoted by iron. Nature 483, 198–200.
Lechler, M., Pogge von Strandmann, P.A.E., Jenkyns, H.C., Prosser, G., Parente, M., 2015. Lithium-isotope evidence for enhanced silicate weathering during OAE 1a (Early Aptian Selli event). Earth Planet. Sci. Lett. 432, 210–222.
Lemarchand, E., Chabaux, F., Vigier, N., Millot, R., Pierret, M.C., 2010. Lithium isotope systematics in a forested granitic catchment (Strengbach, Vosges Mountains, France). Geochim. Cosmochim. Acta 74, 4612–4628.
Li, G., West, A.J., 2014. Evolution of Cenozoic seawater lithium isotopes: coupling of global denudation regime and shifting seawater sinks. Earth Planet. Sci. Lett. 401, 284–293.
Li, S., Gaschnig, R.M., Rudnick, R.L., 2016. Insights into chemical weathering of the upper continental crust from the geochemistry of ancient glacial diamictites. Geochim. Cosmochim. Acta 176, 96–117.
Li, W., Liu, X.-M., Chadwick, O.A., 2020. Lithium isotope behavior in Hawaiian regoliths: soil-atmosphere-biosphere exchanges. Geochim. Cosmochim. Acta 285, 175–192.
Li, W., Liu, X.-M., Wang, K., Koefoed, P., 2021. Lithium and potassium isotope fractionation during silicate rock dissolution: an experimental approach. Chem. Geol. 568, 120142.
Liu, X.-M., Wanner, C., Rudnick, R.L., McDonough, W.F., 2015. Processes controlling δ7Li in rivers illuminated by study of streams and groundwaters draining basalts. Earth Planet. Sci. Lett. 409, 212–224.
Liu, C.-Y., Pogge von Strandmann, P.A.E., Tarbuck, G., Wilson, D.J., 2022. Experimental investigation of oxide leaching methods for Li isotopes. Geostand. Geoanal. Res. 46, 493–518.
Louvat, P., Gislason, S.R., Allegre, C.J., 2008. Chemical and mechanical erosion rates in Iceland as deduced from river dissolved and solid material. Am. J. Sci. 308, 679–726.
Maffre, P., Godderis, Y., Vigier, N., Moquet, J.-S., Carretier, S., 2020. Modelling the riverine δ7Li variability throughout the Amazon Basin. Chem. Geol. 119336.
Millot, R., Vigier, N., Gaillardet, J., 2010. Behaviour of lithium and its isotopes during weathering in the Mackenzie Basin, Canada. Geochim. Cosmochim. Acta 74, 3897–3912.
Murphy, M.J., Porcelli, D., Pogge von Strandmann, P.A.E., Hirst, C.A., Kutscher, L., Katchinoff, J.A., Mörth, C.-M., Maximov, T., Andersson, P.S., 2019. Tracing silicate weathering processes in the permafrost-dominated Lena River watershed using lithium isotopes. Geochim. Cosmochim. Acta 245, 154–171.
Norddahl, H., Petursson, H.G., 2005. Relative Sea level changes in Iceland: New aspects of the Weichselian deglaciation of Iceland. In: Caseldine, C.J., Russell, A., Hardardóttir, J., Knudsen, O. (Eds.), Iceland: Modern Processes, Past Environments. Elsevier, pp. 25–78.
Oskarsdottir, S.M., Gislason, S.R., Snorrason, A., Halldorsdottir, S.G., Gisladottir, G., 2011. Spatial distribution of dissolved constituents in Icelandic river waters. J. Hydrol. 397, 175–190.
Parkhurst, D.L., Appelo, C.A.J., 1999. User's guide to PHREEQC (version 2) - a computer program for speciation, batch-reaction, one-dimensional transport, and inverse geochemical calculations. In: Water-Resouces Investigations.
Pearce, C.R., Burton, K.W., Pogge von Strandmann, P.A.E., James, R.H., Gislason, S.R., 2010. Molybdenum isotope behaviour accompanying continental weathering and riverine transport in a basaltic terrain. Earth Planet. Sci. Lett. 295, 104–114.
Pistiner, J.S., Henderson, G.M., 2003. Lithium-isotope fractionation during continental weathering processes. Earth Planet. Sci. Lett. 214, 327–339.

Pogge von Strandmann, P.A.E., Burton, K.W., James, R.H., van Calsteren, P., Gislason, S. R., Mokadem, F., 2006. Riverine behaviour of uranium and lithium isotopes in an actively glaciated basaltic terrain. Earth Planet. Sci. Lett. 251, 134–147.
Pogge von Strandmann, P.A.E., Burton, K.W., James, R.H., van Calsteren, P., Gislason, S. R., 2008. The influence of weathering processes on riverine magnesium isotopes in a basaltic terrain. Earth Planet. Sci. Lett. 276, 187–197.
Pogge von Strandmann, P.A.E., Burton, K.W., James, R.H., van Calsteren, P., Gislason, S. R., 2010. Assessing the role of climate on uranium and lithium isotope behaviour in rivers draining a basaltic terrain. Chem. Geol. 270, 227–239.
Pogge von Strandmann, P.A.E., Burton, K.W., Porcelli, D., James, R.H., van Calsteren, P., Gislason, S.R., 2011a. Transport and exchange of U-series nuclides between suspended material, dissolved load and colloids in rivers draining basaltic terrains. Earth Planet. Sci. Lett. 301, 125–136.
Pogge von Strandmann, P.A.E., Elliott, T., Marschall, H.R., Coath, C., Lai, Y.J., Jeffcoate, A.B., Ionov, D.A., 2011b. Variations of Li and Mg isotope ratios in bulk chondrites and mantle xenoliths. Geochim. Cosmochim. Acta 75, 5247–5268.
Pogge von Strandmann, P.A.E., Opfergelt, S., Lai, Y.J., Sigfusson, B., Gislason, S.R., Burton, K.W., 2012. Lithium, magnesium and silicon isotope behaviour accompanying weathering in a basaltic soil and pore water profile in Iceland. Earth Planet. Sci. Lett. 339–340, 11–23.
Pogge von Strandmann, P.A.E., Jenkyns, H.C., Woodfine, R.G., 2013. Lithium isotope evidence for enhanced weathering during Oceanic Anoxic Event 2. Nat. Geosci. 6, 668–672.
Pogge von Strandmann, P.A.E., Porcelli, D., James, R.H., van Calsteren, P., Schaefer, B.F., Cartwright, I., Reynolds, B.C., Burton, K.W., 2014. Chemical weathering processes in the Great Artesian Basin: evidence from lithium and silicon isotopes. Earth Planet. Sci. Lett. 406, 24–36.
Pogge von Strandmann, P.A.E., Burton, K.W., Opfergelt, S., Eiriksdottir, E.S., Murphy, M. J., Einarsson, A., Gislason, S.R., 2016. The effect of hydrothermal spring weathering processes and primary productivity on lithium isotopes: Lake Myvatn, Iceland. Chem. Geol. 445, 4–13.
Pogge von Strandmann, P.A.E., Frings, P.J., Murphy, M.J., 2017a. Lithium isotope behaviour during weathering in the Ganges Alluvial Plain. Geochim. Cosmochim. Acta 198, 17–31.
Pogge von Strandmann, P.A.E., Desrochers, A., Murphy, M.J., Finlay, A.J., Selby, D., Lenton, T.M., 2017b. Global climate stabilisation by chemical weathering during the Hirnantian glaciation. GPL 3, 230–237.
Pogge von Strandmann, P.A.E., Hendry, K.R., Hatton, J.E., Robinson, L.F., 2019a. The response of magnesium, silicon, and calcium isotopes to rapidly uplifting and weathering terrains: South Island, New Zealand. Front. Earth Sci. 7.
Pogge von Strandmann, P.A.E., Fraser, W.T., Hammond, S.J., Tarbuck, G., Wood, I.G., Oelkers, E.H., Murphy, M.J., 2019b. Experimental determination of Li isotope behaviour during basalt weathering. Chem. Geol. 517, 34–43.
Pogge von Strandmann, P.A.E., Kasemann, S.A., Wimpenny, J.B., 2020. Lithium and lithium isotopes in earth's surface cycles. Elements 16, 253–258.
Pogge von Strandmann, P.A.E., Dellinger, M., West, A.J., 2021a. Lithium Isotopes: A Tracer of Past and Present Silicate Weathering. Cambridge University Press.
Pogge von Strandmann, P.A.E., Renforth, P., West, A.J., Murphy, M.J., Luu, T.-H., Henderson, G.M., 2021b. The lithium and magnesium isotope signature of olivine dissolution in soil experiments. Chem. Geol. 560, 120008.
Pogge von Strandmann, P.A.E., Burton, K.W., Opfergelt, S., Genson, B., Guicharnaud, R. A., Gislason, S.R., 2021c. The lithium isotope response to the variable weathering of soils in Iceland. Geochim. Cosmochim. Acta 313, 55–73.
Pogge von Strandmann, P.A.E., Jones, M.T., West, A.J., Murphy, M.J., Stokke, E.W., Tarbuck, G., Wilson, D.J., Pearce, C.R., Schmidt, D.N., 2021d. Lithium isotope evidence for enhanced weathering and erosion during the Paleocene-Eocene Thermal Maximum. Sci. Adv. 7, eabh4224.
Pogge von Strandmann, P.A.E., Liu, X., Liu, C.Y., Wilson, D.J., Hammond, S.J., Tarbuck, G., Aristilde, L., Krause, A.J., Fraser, W.T., 2022. Lithium isotope behaviour during basalt weathering experiments amended with organic acids. Geochim. Cosmochim. Acta 328, 37–57.
Ramos, E.J., Breecker, D.O., Barnes, J.D., Li, F., Gingerich, P.D., Loewy, S.L., Satkoski, A. M., Baczynski, A.A., Wing, S.L., Miller, N.R., Lassiter, J.C., 2022. Swift weathering response on floodplains during the Paleocene-Eocene Thermal Maximum. Geophys. Res. Lett. 49 e2021GL097436.
Ryan, J.G., Kyle, P.R., 2004. Lithium abundance and lithium isotope variations in mantle sources: insights from intraplate volcanic rocks from Ross Island and Marie Byrd Land (Antarctica) and other oceanic islands. Chem. Geol. 212, 125–142.
Snæbjörnsdóttir, S.O., Gislason, S.R., Galeczka, I.M., Oelkers, E.H., 2018. Reaction path modelling of in-situ mineralisation of CO2 at the CarbFix site at Hellisheidi, SW-Iceland. Geochim. Cosmochim. Acta 220, 348–366.
Sproson, A.D., Pogge von Strandmann, P.A.E., Selby, D., Jarochowska, E., Fryda, J., Hladil, J., Loydell, D.K., Slavik, L., Calner, M., Maier, G., Munnecke, A., Lenton, T. M., 2022. Osmium and lithium isotope evidence for weathering feedbacks linked to orbitally paced organic carbon burial and Silurian glaciations. Earth Planet. Sci. Lett. 577, 117260.
Stefansson, A., Gislason, S.R., 2001. Chemical weathering of basalts, Southwest Iceland: effect of rock crystallinity and secondary minerals on chemical fluxes to the ocean. Am. J. Sci. 301, 513–556.
Steinhoefel, G., Brantley, S.L., Fantle, M.S., 2021. Lithium isotopic fractionation during weathering and erosion of shale. Geochim. Cosmochim. Acta 295, 155–177.
Thordarson, T., Hoskuldsson, A., 2002. Iceland. Terra Publishing.
Tipper, E.T., Stevenson, E.I., Alcock, V., Knight, A.C.G., Baronas, J.J., Hilton, R.G., Bickle, M.J., Larkin, C.S., Feng, L., Relph, K.E., Hughes, G., 2021. Global silicate weathering flux overestimated because of sediment–water cation exchange. Proc. Natl. Acad. Sci. 118, e2016430118.
Verney-Carron, A., Vigier, N., Millot, R., Hardarsson, B.S., 2015. Lithium isotopes in hydrothermally altered basalts from Hengill (SW Iceland). Earth Planet. Sci. Lett. 411, 62–71.
Vigier, N., Decarreau, A., Millot, R., Carignan, J., Petit, S., France-Lanord, C., 2008. Quantifying Li isotope fractionation during smectite formation and implications for the Li cycle. Geochim. Cosmochim. Acta 72, 780–792.
Vigier, N., Gislason, S.R., Burton, K.W., Millot, R., Mokadem, F., 2009. The relationship between riverine lithium isotope composition and silicate weathering rates in Iceland. Earth Planet. Sci. Lett. 287, 434–441.
Walker, J.C.G., Hays, P.B., Kasting, J.F., 1981. A negative feedback mechanism for the long-term stabilization of earths surface-temperature. J. Geophys. Res. Oceans Atmos. 86, 9776–9782.
Wanner, C., Sonnenthal, E.L., Liu, X.-M., 2014. Seawater δ7Li: a direct proxy for global CO2 consumption by continental silicate weathering? Chem. Geol. 381, 154–167.
Wei, G.-Y., Wei, W., Wang, D., Li, T., Yang, X., Shields, G.A., Zhang, F., Li, G., Chen, T., Yang, T., Ling, H.-F., 2020. Enhanced chemical weathering triggered an expansion of euxinic seawater in the aftermath of the Sturtian glaciation. Earth Planet. Sci. Lett. 539, 116244.
Wilson, D.J., Pogge von Strandmann, P.A.E., White, J., Tarbuck, G., Marca, A.D., Atkinson, T.C., Hopley, P.J., 2021. Seasonal variability in silicate weathering signatures recorded by Li isotopes in cave drip-waters. Geochim. Cosmochim. Acta 312, 194–216.
Wimpenny, J., Gislason, S.R., James, R.H., Gannoun, A., Pogge von Strandmann, P.A.E., Burton, K.W., 2010. The behaviour of Li and Mg isotopes during primary phase dissolution and secondary mineral formation in basalt. Geochim. Cosmochim. Acta 74, 5259–5279.
Wimpenny, J., Colla, C.A., Yu, P., Yin, Q.Z., Rustad, J.R., Casey, W.H., 2015. Lithium isotope fractionation during uptake by gibbsite. Geochim. Cosmochim. Acta 168, 133–150.
Winnick, M.J., Druhan, J.L., Maher, K., 2022. Weathering intensity and lithium isotopes: a reactive tracport perspective. Am. J. Sci. 322, 647–682.
Yin, Y.-S., Wei, G.-Y., Pogge von Strandmann, P.A.E., Lechte, M.A., Hohl, S.V., Lin, Y.-B., Li, D., Chen, T., Yang, T., Zhang, F., Isson, T.T., Zhang, H., Cai, Y., Ling, H.-F., 2023. Widespread clay authigenesis and highly congruent silicate weathering in the Marinoan aftermath. Earth Planet. Sci. Lett. 623, 118423.
Zhang, J.-W., Zhao, Z.-Q., Yan, Y.-N., Cui, L.-F., Wang, Q.-L., Meng, J.-L., Li, X.-D., Liu, C.-Q., 2021. Lithium and its isotopes behavior during incipient weathering of granite in the eastern Tibetan Plateau, China. Chem. Geol. 559, 119969.
Zhang, F., Dellinger, M., Hilton, R.G., Yu, J., Allen, M.B., Densmore, A.L., Sun, H., Jin, Z., 2022. Hydrological control of river and seawater lithium isotopes. Nat. Commun. 13, 3359.